Spin-flip effects on the supercurrent through mesoscopic superconducting junctions

2005 J. Phys.: Condens. Matter 17 5207

(http://iopscience.iop.org/0953-8984/17/34/005)

INSTITUTE OF PHYSICS PUBLISHING JOURNAL OF PHYSICS: CONDENSED MATTER

J. Phys.: Condens. Matter **17** (2005) 5207–5214 doi:10.1088/0953-8984/17/34/005

Spin-flip effects on the supercurrent through mesoscopic superconducting junctions

Hui Pan[1,2] **and Tsung-Han Lin**[2]

[1] Department of Physics, Beijing University of Aeronautics and Astronautics, Beijing 100083, People's Republic of China
[2] State Key Laboratory for Mesoscopic Physics and Department of Physics, Peking University, Beijing 100871, People's Republic of China

Received 20 May 2005
Published 12 August 2005
Online at stacks.iop.org/JPhysCM/17/5207

Abstract

We investigate the spin-flip effects on the Andreev bound states and the supercurrent in a superconductor/quantum-dot/superconductor system, theoretically. The spin-flip scattering in the quantum dot can reverse the supercurrent flowing through the system, which results in a π-junction transition. By controlling the energy level of the quantum dot, the π-junction transition can be caused to occur again. The two mechanisms of the π-junction transitions are interpreted within the picture of Andreev bound states.

1. Introduction

The superconductor coupled mesoscopic hybrid systems have attracted much attention in recent years, not only because of their fundamental interest, but also of because potential applications in future nanoelectronics [1–4]. In ballistic superconductor/normal-metal/superconductor (S/N/S) junctions, Andreev bound states can be formed [5]. Each Andreev bound state carries a supercurrent in the positive or negative direction at a given phase difference ϕ between the two superconductors. Therefore, the net supercurrent between two superconductors depends not only on the phase difference ϕ, but also on the occupation of the Andreev bound states. When two superconductors are weakly linked, the current–phase relation is $I = I_c \sin(\phi)$. On some occasions, the sign of I_c may be reversed [6], which is referred to as a π-junction transition, because the minus sign can be absorbed into the phase factor as $\sin(\phi + \pi)$.

The spin–orbit interaction plays an important role in the quantum dot (QD), because it can change the spin orientation of an electron. The spin–orbit interaction can couple the spin degree of freedom and the orbital motion of an electron, which provides a useful way to manipulate and control the electron spin. The spin-flip mechanisms in the GaAs-based QD have already been studied [7]. This research direction is expanding at a very rapid pace due to its possible applications to spintronics. Recently, the spin-flip effects on transport properties of a quantum dot in the normal-metal and superconductor hybrid system has been

studied [8]. Various resonant peaks appear for the different spin-flip strengths in the QD. The spin-dependent Andreev reflection tunnelling through a QD with spin-flip scattering has also been studied [9]. It is found that competition between the intradot spin-flip scattering and the tunnelling coupling to the leads dominates the resonant behaviours of the Andreev reflection.

It is natural to ask whether the intradot spin-flip scattering could induce some novel phenomena in the supercurrent. Motivated by this, we investigate the spin-flip scattering effects on the supercurrent and Andreev bound states in the superconductor/quantum-dot/superconductor (S/QD/S) system in this paper. By using standard nonequilibrium Green function (NGF) techniques [10–13], we have analysed quantum transport properties of the S/QD/S system. The spin-flip scattering in an isolated QD can split one spin-degenerate level of the QD into two spin-coherent levels, whose states are a superposition of the spin-up and spin-down ones. This will bring about some novel resonant features in the quantum transport properties of the system. The configuration of the Andreev bound states depends heavily on the spin-flip strength. Since the supercurrent is carried by these states, the spin-flip scattering has a great influence on the amplitude and sign of the supercurrent. The dependence of the supercurrent and Andreev bound states on the gate voltage is also studied.

2. Physical model and formula

The S/QD/S system under consideration is described by the following Hamiltonian:

$$H = \sum_{\alpha=\mathrm{L,R}} H_\alpha + H_{\mathrm{dot}} + H_{\mathrm{T}}, \tag{1}$$

with

$$\begin{aligned} H_\alpha &= \sum_{k,\sigma} \epsilon_{\alpha,k} a^\dagger_{\alpha,k\sigma} a_{\alpha,k\sigma} + \sum_k [\Delta \mathrm{e}^{-\mathrm{i}\phi_\alpha} a^\dagger_{\alpha,k\uparrow} a^\dagger_{\alpha,-k\downarrow} + \mathrm{H.c.}], \\ H_{\mathrm{dot}} &= \sum_\sigma \epsilon_0 d^\dagger_\sigma d_\sigma + r(d^\dagger_\uparrow d_\downarrow + d^\dagger_\downarrow d_\uparrow), \\ H_{\mathrm{T}} &= \sum_{\alpha,k\sigma} [t_\alpha a^\dagger_{\alpha,k\sigma} d_\sigma + \mathrm{H.c.}], \end{aligned} \tag{2}$$

where H_α ($\alpha = \mathrm{L/R}$) is the standard BCS Hamiltonian for the left/right superconducting leads with phase $\phi_{\mathrm{L}}/\phi_{\mathrm{R}}$ and the energy gap Δ. H_{dot} models the quantum dot with a single spin-degenerate level ϵ_0, which can be controlled by the gate voltage. The spin-flip term in the H_{dot} comes from the spin–orbit interaction in the quantum dot. H_{T} denotes the tunnelling part of the Hamiltonian and $t_{\mathrm{L,R}}$ are the hopping matrices. The supercurrent can be calculated from standard NGF techniques.

The 4×4 Nambu representation is used to include the physics of AR and the spin-flip process in a unified formalism. The retarded Green function is defined as $G^r_{\alpha,\beta}(t,t') = \mp \mathrm{i}\theta(\pm t \mp t')\langle\{\Psi_\alpha(t), \Psi^\dagger_\beta(t')\}\rangle$ with the operator $\Psi_\alpha = (\psi^\dagger_{\alpha\uparrow}, \psi_{\alpha\downarrow}, \psi^\dagger_{\alpha\downarrow}, \psi_{\alpha\uparrow})^\dagger$. Let g^r and G^r denote the Fourier-transformed retarded Green function of the QD without and with the coupling to the leads. In the Nambu representation, they can be written as

$$(g^r(\epsilon))^{-1} = \begin{pmatrix} \epsilon - \epsilon_0 + \mathrm{i}0^+ & 0 & -r & 0 \\ 0 & \epsilon + \epsilon_0 + \mathrm{i}0^+ & 0 & r \\ -r & 0 & \epsilon - \epsilon_0 + \mathrm{i}0^+ & 0 \\ 0 & r & 0 & \epsilon + \epsilon_0 + \mathrm{i}0^+ \end{pmatrix}. \tag{3}$$

The retarded self-energy under the wide-bandwidth approximation can be derived as [12, 13]

$$\Sigma^r_{\mathrm{L/R}}(\epsilon) = -\mathrm{i}\Gamma_{\mathrm{L/R}}\rho(\epsilon)\begin{pmatrix} 1 & -\frac{\Delta}{\epsilon}\mathrm{e}^{-\mathrm{i}\phi_{\mathrm{L/R}}} & 0 & 0 \\ -\frac{\Delta}{\epsilon}\mathrm{e}^{\mathrm{i}\phi_{\mathrm{L/R}}} & 1 & 0 & 0 \\ 0 & 0 & 1 & \frac{\Delta}{\epsilon}\mathrm{e}^{-\mathrm{i}\phi_{\mathrm{L/R}}} \\ 0 & 0 & \frac{\Delta}{\epsilon}\mathrm{e}^{\mathrm{i}\phi_{\mathrm{L/R}}} & 1 \end{pmatrix}, \quad (4)$$

where $\Gamma_{\mathrm{L/R}}$ are the appropriate linewidth functions describing the coupling between the dot and the respective superconducting leads. Under the wide-bandwidth approximation, the linewidth functions are independent on the energy variable. Furthermore, we set $\phi_{\mathrm{L}} = \phi/2$ and $\phi_{\mathrm{R}} = -\phi/2$, $\Gamma_{\mathrm{L}} = \Gamma_{\mathrm{R}} = \Gamma$ with small values for the symmetric and weak-coupling case. The factor $\rho(\epsilon)$ is defined as

$$\rho(\epsilon) = \begin{cases} \dfrac{|\epsilon|}{(\epsilon^2 - \Delta^2)} & |\epsilon| > \Delta \\ \dfrac{|\epsilon|}{\mathrm{i}(\Delta^2 - \epsilon^2)} & |\epsilon| < \Delta. \end{cases} \quad (5)$$

By using the Dyson equation, the retarded Green function of the system can be obtained as

$$G^r(\epsilon) = [g^{r^{-1}}(\epsilon) - \Sigma^r(\epsilon)]^{-1}, \quad (6)$$

where $\mathbf{\Sigma}^r = \mathbf{\Sigma}^r_{\mathrm{L}} + \mathbf{\Sigma}^r_{\mathrm{R}}$. The Josephson current is expressed as

$$I_{\mathrm{L/R}} = I_{\mathrm{L/R},\uparrow} + I_{\mathrm{L/R},\downarrow} = \frac{2e}{\hbar}\int \frac{\mathrm{d}\epsilon}{2\pi}\,\mathrm{Tr}\{\hat{\sigma}_z\,\mathrm{Re}[G\Sigma_{\mathrm{L/R}}]^<\}, \quad (7)$$

where $[AB]^< \equiv A^<B^a + A^rB^<$ and $\hat{\sigma}_z$ is a 4×4 matrix with the Pauli matrices σ_z as its diagonal components. In the steady transport, the current is

$$I = \tfrac{1}{2}(I_{\mathrm{L}} - I_{\mathrm{R}}) = \frac{e}{\hbar}\int \frac{\mathrm{d}\epsilon}{2\pi} j(\epsilon) = \frac{e}{\hbar}\int \frac{\mathrm{d}\epsilon}{2\pi}\,\mathrm{Tr}\{\hat{\sigma}_z\,\mathrm{Re}[G(\Sigma_{\mathrm{L}} - \Sigma_{\mathrm{R}})]^<\}. \quad (8)$$

Applying the fluctuation-dissipation theorem, one has

$$G^<(\epsilon) = f(\epsilon)(G^a(\epsilon) - G^r(\epsilon)), \qquad \Sigma^<_{\mathrm{L/R}} = f(\epsilon)(\Sigma^a_{\mathrm{L/R}} - \Sigma^r_{\mathrm{L/R}}), \quad (9)$$

where $f(\epsilon) = 1/(\mathrm{e}^{\beta\epsilon} + 1)$ is the Fermi distribution function. Consequently, the Josephson current is expressed as

$$I = \frac{e}{\hbar}\int \frac{\mathrm{d}\epsilon}{2\pi} f(\epsilon) j(\epsilon), \quad (10)$$

in which the current density $j(\epsilon)$ is defined as

$$j(\epsilon) = \mathrm{Tr}\{\hat{\sigma}_z\,\mathrm{Re}[G^a(\Sigma^a_{\mathrm{L}} - \Sigma^a_{\mathrm{R}}) - G^r(\Sigma^r_{\mathrm{L}} - \Sigma^r_{\mathrm{R}})]\}. \quad (11)$$

The analysis of the current carrying spectrum $j(\epsilon)$ provides the information on the supercurrent carried by each of the Andreev bound states. The Josephson current can be divided into two parts, contributed by the continuous spectrum for $|\omega| > \Delta$ and the discrete spectrum for $|\omega| < \Delta$:

$$\begin{aligned} I &= I_{\mathrm{c}} + I_{\mathrm{d}}, \\ I_{\mathrm{c}} &= \frac{e}{\hbar}\left(\int_{-\infty}^{-\Delta} + \int_{\Delta}^{\infty}\right)\frac{\mathrm{d}\epsilon}{2\pi} f(\epsilon) j(\epsilon), \\ I_{\mathrm{d}} &= \frac{e}{\hbar}\int_{-\Delta}^{\Delta}\frac{\mathrm{d}\epsilon}{2\pi} f(\epsilon) j(\epsilon). \end{aligned} \quad (12)$$

The averaged LDOS is given by

$$D(\epsilon) = -\frac{1}{\pi}\,\mathrm{Tr}\{\mathrm{Im}[G^r(\epsilon)]\}. \quad (13)$$

We perform the calculations at zero temperature in units of $\hbar = e = 1$. The energy gap of the superconductor is fixed as $\Delta = 1$. All the energy quantities in the calculations are scaled by Δ. The linewidth is $\Gamma = 0.1\Delta$ for the symmetric and weak-coupling case.

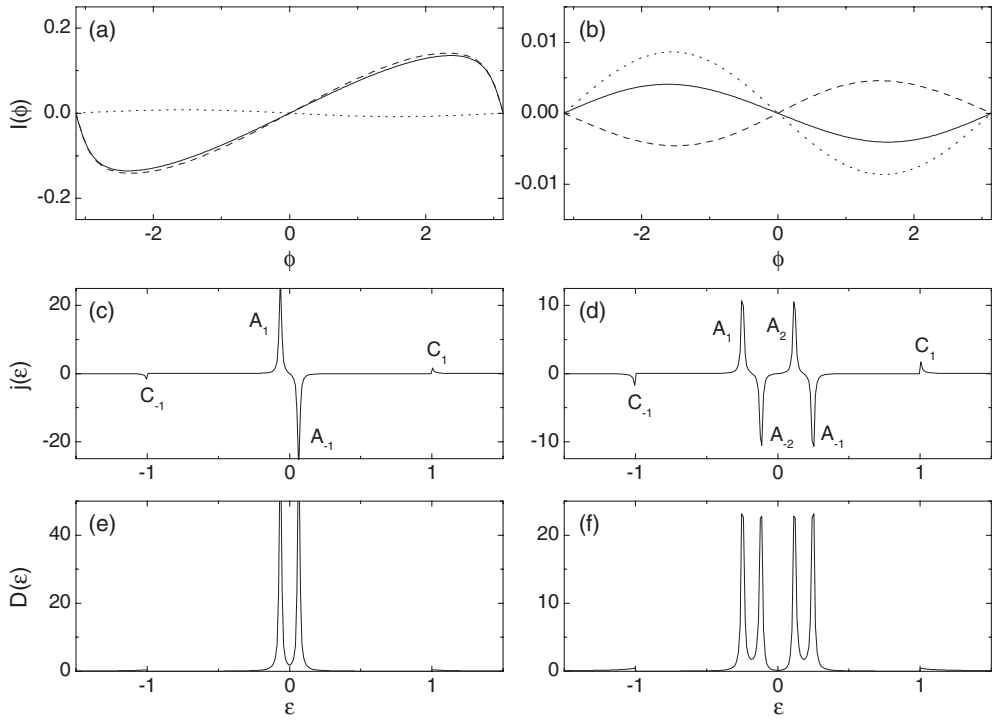

Figure 1. The current I (solid line), I_d (dashed line) and I_c (dotted line) versus ϕ for $r = 0$ (a) and $r = 0.2$ (b) with the dot level $\epsilon_0 = 0$. (c) and (d) are the corresponding $j(\epsilon)$, and (e) and (f) are the corresponding $D(\epsilon)$, respectively.

3. Results and discussion

In the following, the numerical results on the supercurrents and the Andreev quasibound states are discussed in detail. The supercurrent originates from Andreev reflection at the interface between the superconducting leads and the central region. Figures 1(a) and (b) present the supercurrent I (which includes both I_c and I_d) versus the phase difference ϕ with different spin-flip scattering strengths r. First, we investigate the case without the spin-flip scattering, $r = 0$. The current I_d from the discrete spectrum versus ϕ is similar to a $\sin(\phi)$-like curve. However, the current I_c from the continuous spectrum versus ϕ is similar to a $\sin(\phi + \pi)$-like curve, because the current I_c follows a π-junction Josephson relation [14, 15]. Furthermore, the current I_d is much larger than the current I_c, which means that the total supercurrent I is mainly contributed by I_d and also shows a sine-like dependence on the phase ϕ. Now, we investigate the case with the spin-flip scattering $r = 0.2$. It is interesting to note that I versus ϕ is not a $\sin(\phi)$-like but a $\sin(\phi + \pi)$-like curve. There is a π-junction transition for the supercurrent–phase relation. The reason is related to the spin-flip scattering which greatly suppresses the current I_d. Thus the total supercurrent is mainly contributed by I_c but not by I_d, like in the case without the spin-flip scattering. Due to the quite different dependences of I_c and I_d on ϕ, the supercurrent I shows a π-junction transition under the influence of the spin-flip scattering effects.

To fully understand the π-junction transition, we plot the $j(\epsilon)$ for the cases with and without the spin-flip scattering in figures 1(c) and (d). For the case with $r = 0$, the original

level $\epsilon_0 = 0$ is split into two Andreev quasibound states. When the energy ϵ of an incoming electron lines up with the Andreev bound states, a resonance occurs, leading to a very large supercurrent. As seen from figure 1(c), $j(\epsilon)$ has two δ-function-type discrete spectra within the superconducting gap, corresponding to the two Andreev bound states. They carry supercurrents with opposite signs: positive for A_1 and negative for A_{-1}. $j(\epsilon)$ also has a continuous spectrum outside the superconducting gap: negative for C_{-1} and positive for C_1. At zero temperature, only the spectrum of $\epsilon < 0$ relates to the current. Since the contribution from the discrete spectrum A_1 is much larger than that from the continuous one C_{-1}, the current I is mostly contributed by I_d. For the case with $r = 0.2$, the original level $\epsilon_0 = 0$ is split into two, ϵ_{01} and ϵ_{02}, due to the spin-flip perturbation, which results in four Andreev bound states. The original Andreev bound state A_1 is split into two, A_1 and A_2, and similarly A_{-1} is split into A_{-1} and A_{-2}. $j(\epsilon)$ has four δ-function-type discrete spectra within the superconducting gap. The Andreev bound states depend strongly on the configuration of the QD levels (ϵ_{01},ϵ_{02}), but weakly on the phase difference ϕ, and the electron levels ϵ_{01} and ϵ_{02} are coupled by Andreev reflection tunnelling. Therefore, Andreev bound states can be viewed as hybrids of ϵ_{01} and ϵ_{02}. With increasing r, A_1 and A_{-2} move in the same direction, and both of them are below the Fermi level at strong enough r. As a consequence, they make little net contribution to the supercurrent, and the relatively small negative continuous spectrum of C_{-1} dominates. The contribution from the discrete spectrum is suppressed by the spin-flip scattering. This is the origin of the π-junction transition in the supercurrent under the influence of the spin-flip scattering in the QD. Another important quantity, the local density of states (LDOS) $D(\epsilon)$, is also shown in figures 1(e) and (f). A series of very narrow peaks emerge in $D(\epsilon)$, clearly indicating the formation of Andreev quasibound states inside the QD. The peaks of the current density $j(\epsilon)$ are located precisely at the energies of Andreev bound states, which is a clear indication that the current is carried by these states.

The results above are obtained by fixing the intradot level ϵ_0 to zero, which is just at the centre of the gap and at the Fermi level of both left and right leads. Next, we investigate how the supercurrent is affected when ϵ_0 is moved away from zero by the gate voltage. The supercurrent and the corresponding current density and LDOS at some nonzero ϵ_0 are plotted in figure 2. As seen from figure 2(a), $I(\phi)$ at $\epsilon_0 = 0.3$ is quite different from that at $\epsilon_0 = 0$ in figure 1(b). It is noted that a π-junction transition occurs, and then the supercurrent has $\sin(\phi)$-like phase dependence similar to that in figure 1(a). To explain this transition, the corresponding current density $j(\epsilon)$ is also shown in figure 2(b). With $\epsilon_0 \neq 0$, the Andreev quasibound states in $j(\epsilon)$ are shifted in their positions. The two successive states are shifted in opposite directions. The two bound states A_1 and A_2 carrying the positive current move to $-\Delta$, while A_{-1} and A_{-2} carrying the negative current move to Δ. At small ϵ_0, the net current from discrete spectra A_1 and A_{-2} are very small and the continuous spectrum C_{-1} mainly contributes the current. At large enough ϵ_0, the positions of A_2 and A_{-2} can even move past, over the Fermi level, and both of these positions are below the Fermi level. Now, the currents are mainly contributed by the discrete spectra of A_1 and A_2, and not by C_{-1} any longer. This is exactly why the π-junction transition occurs. The corresponding $D(\epsilon)$ shown in figure 2(c) is symmetric about the Fermi level. The narrow peaks with different height clearly indicate the shift of the Andreev bound states.

To clearly show the π-junction transitions mentioned above, the dependences of $I(\phi = \pi/2)$ on r and ϵ_0 are plotted in figure 3. As shown in figure 3(a), $I(\pi/2)$ decreases slowly at first with increasing r. When the spin-flip scattering strength r is comparable and close to ϵ_0, $I(\pi/2)$ decreases rapidly and can even change sign from positive to negative. Then the π-phase transition occurs as shown in figure 1. At larger ϵ_0, a stronger r is needed to move the bound state A_{-2} to below the Fermi level like A_1. The negative current carried by A_{-2} counteracts

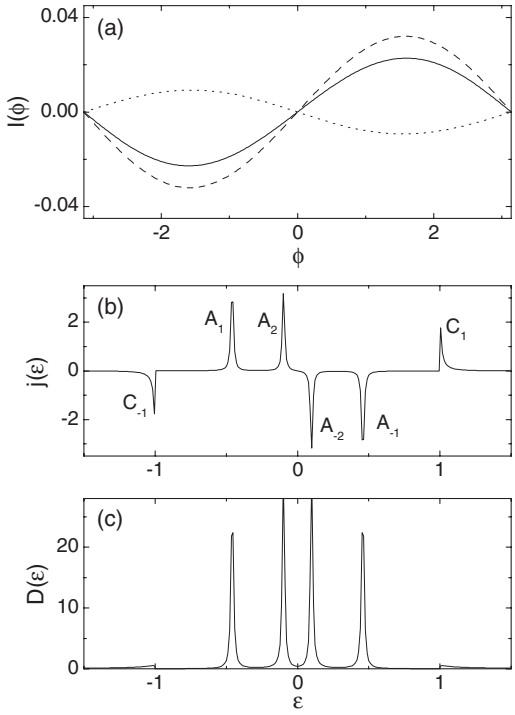

Figure 2. The current I (solid line), I_d (dashed line) and I_c (dotted line) versus ϕ for $\epsilon_0 = 0.3$ (a) with the spin-flip scattering strength $r = 0.2$. (b) and (c) are the corresponding $j(\epsilon)$ and $D(\epsilon)$, respectively.

the positive current carried by A_1. Then the π-junction transition can occur. When there is no spin-flip scattering $r = 0$, increasing ϵ_0 can decrease $I(\pi/2)$ as shown in figure 3(b). Because the intradot energy levels ϵ_{01} and ϵ_{02} are not symmetric about the Fermi level at nonzero ϵ_0, the Andreev reflections are suppressed and thus the current decreases. For the nonzero r, $I(\pi/2)$ first increases and then decreases. At small spin-flip strength r, increasing ϵ_0 does not change of the sign of $I(\pi/2)$. At some strong enough r, which already induces a π-junction transition, $I(\pi/2)$ can change sign from negative to positive with increasing ϵ_0. Then another π-phase transition occurs as shown in figure 2. When ϵ_0 is comparable and close to r, a maximum of $I(\pi/2)$ appears. The reason is related to the position shift of the Andreev bound states with ϵ_0 as mentioned above. With increasing ϵ_0, A_1 and A_2 move to below the Fermi level while A_{-1} and A_{-2} move to above the Fermi level. The components contributed to the supercurrent change from (A_1, A_{-2}, C_{-1}) to (A_1, A_2, C_{-1}), and then the current at first increases. With further increasing ϵ_0, the current density is suppressed greatly due to the asymmetry of the intradot levels, and then the current decreases again.

4. Conclusion

In summary, by using the nonequilibrium Green function method, the spin-flip scattering effects on the supercurrent and Andreev bound states are studied in detail. The supercurrent is mostly contributed by the discrete Andreev bound states if there is no spin-flip scattering. The original Andreev bound state is split into two, due to the spin-flip scattering, and the

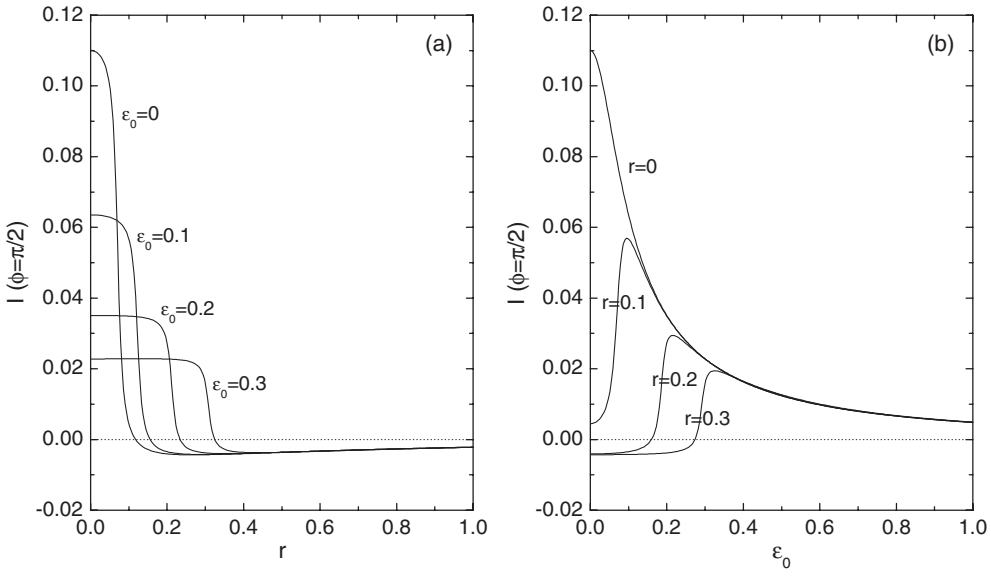

Figure 3. (a) The current $I(\pi/2)$ versus r at different $\epsilon_0 = 0$, 0.1, 0.2 and 0.3. (b) The current $I(\pi/2)$ versus ϵ_0 at different $r = 0$, 0.1, 0.2 and 0.3, respectively.

two successive bound states carrying currents with opposite signs move in the same direction with increasing spin-flip scattering strength. The main contributions to the supercurrent can be changed from the discrete spectrum to the continuous spectrum at the appropriate spin-flip scattering strength, which results in a π-junction transition. Furthermore, another π-junction transition can appear if the intradot energy level is controlled to some appropriate value by the gate voltage, because the two successive bound states carrying currents with the same signs move in the same direction. The main contributions to the supercurrent are from the discrete spectrum again, which results in this transition. Although the strength of the spin-flip scattering and the position of the intradot energy level have quite different influences on the supercurrent, the two π-junction transition mechanisms are involved in the change of the current density. The spin-flip scattering provides us with a new way to realize the π-junction transition of the supercurrent. We hope that the theoretical predictions may have practical applications in future nanoelectronics.

Acknowledgment

This project was supported by the State Key Laboratory for Mesoscopic Physics in Peking University.

References

[1] Ralph D C, Black C T and Tinkham M 1995 *Phys. Rev. Lett.* **74** 3241
[2] Knorr N, Schneider M A, Diekhoner L, Wahl P and Kern K 2002 *Phys. Rev. Lett.* **88** 096804
[3] Buitelaar M R, Nussbaumer T and Schönenberger C 2002 *Phys. Rev. Lett.* **89** 256801
[4] Takayanagi H, Akazaki T and Nitta J 1995 *Phys. Rev. Lett.* **75** 3533
[5] Bagwell P F 1992 *Phys. Rev.* B **46** 12573
[6] Baselmans J J A, Morpurgo A F, van Wees B J and Klapwijk T M 1999 *Nature* **397** 43

[7] Khaetskii A V and Nazarov Y V 2000 *Phys. Rev.* B **61** 12639
Khaetskii A V 2001 *Physica* E **10** 27
[8] Chen Z, Wang J, Wang B and Xing D Y 2005 *Phys. Lett.* A **334** 436
[9] Cao X, Shi Y, Song X, Zhou S and Chen H 2004 *Phys. Rev.* B **70** 235341
[10] Yeyati A L, Martin-Rodero A and Cruvas J C 1996 *Phys. Rev.* B **54** 7366
[11] Yeyati A L, Cuevas J C, Lopee-Davalos A and Martin-Rodero A 1999 *Phys. Rev.* B **55** R6137
[12] Sun Q F, Wang J and Lin T H 2000 *Phys. Rev.* B **62** 648
[13] Sun Q F, Guo H and Wang J 2002 *Phys. Rev.* B **65** 075315
[14] Mühge Th *et al* 1996 *Phys. Rev. Lett.* **77** 1857
[15] van Harlingen D J 1995 *Rev. Mod. Phys.* **67** 515